

## Article

# Study of Solidifying Surplus Sludge as Building Material Using Ordinary Portland Cement

Jiling Liang , Han He, Jianwei Wei, Tingting Han, Wenwu Wang, Lu Wang, Jie Han, Lunqiu Zhang, Yan Zhang and Haiqiang Ma

College of Civil Engineering, Liaoning Petrochemical University, Fushun 113001, China

\* Correspondence: l2j418@126.com; Tel.: +86-183-4131-1292

**Abstract:** In an attempt to effectively utilize a multitude of surplus sludge from sewage treatment plants, ordinary Portland cement was used to solidify the dry surplus sludge as a building material. The dry surplus sludge and cement were mixed at different proportions with a certain dosage of water and then cured for 3–60 days at room temperature. The unconfined compression strength ( $R_C$ ) of solidified blocks was investigated with respect to the effects of the ratio of liquid to solid ( $R_{l/s}$ ), surplus sludge dosage ( $D_S$ ), the dosage of sodium silicate ( $D_{Na_2SiO_3}$ ), and the proportion of fly ash ( $W_F$ ). The fabricated solidified blocks were characterized by scanning electron microscopy (SEM), Fourier transform-infrared spectroscopy (FT-IR), and X-ray Diffraction Analysis (XRD). The results demonstrated that  $R_C$  at 60 days reduced obviously with the increase in  $R_{l/s}$  when  $D_S$  was given, whereas  $R_C$  reduced with  $D_S$  increased to 15.0 wt% from 5.0 wt% for solidified blocks. When  $D_S$  was 5.0 wt%,  $R_C$  of 28 days was reduced from 20.87 MPa to 14.50 MPa, with an increase in  $R_{l/s}$  from 0.35 to 0.55. For the given  $R_{l/s}$ , such as  $R_{l/s} = 0.35$ ,  $R_C$  at 60 days was 23.75 MPa, 2.80 MPa, and 2.50 MPa when  $D_S$  were 5.0 wt%, 10.0 wt%, and 15.0 wt%, respectively, which were relatively lower in comparison to that of Portland cement solidified blocks without surplus sludge (51.40 MPa). In addition, the addition of  $Na_2SiO_3$  and fly ash was favorable in terms of improving the  $R_C$  for solidified blocks.  $R_C$  of 60 days increased initially and then reduced with the increase in  $D_{Na_2SiO_3}$  from 0.0 wt% to 9.0 wt% at  $R_{l/s} = 0.45$  and  $D_S = 5.0$  wt%. At  $D_{Na_2SiO_3} = 7.5$  wt%,  $R_{l/s} = 0.45$ , and  $D_S = 5.0$  wt%, the highest  $R_C$  value of 34.70 MPa was achieved after being cured for 60 days. Furthermore,  $R_C$  of 60 days increased initially and then reduced with  $W_F$  increasing from 0.0 wt% to 25.0 wt%, and the highest  $R_C$  value of 34.35 MPa was achieved at  $W_F = 10.0$  wt%,  $R_{l/s} = 0.45$ , and  $D_S = 5.0$  wt%. At the ratio of  $D_{Na_2SiO_3} = 7.50$  wt%,  $R_{l/s} = 0.35$ ,  $W_F = 20$  wt%,  $D_S = 15.0$  wt% and  $M = 1.00$ ,  $R_C$  of 28 days reached 26.70 MPa. With these values, the utilization of sludge utilized ( $D_S = 15.0$  wt%) was increased by double compared with  $D_S = 5.0$  wt% (20.87 MPa). To investigate the effect of environmental temperature on the mechanical properties and mass of solidified blocks, the freeze-thaw cycling experiment was carried out. The  $R_C$  of 28 days and the mass of the solidified block reduced with the number of freeze-thaw cycles, increasing for solidified blocks with  $D_S$  of 5.0 wt%, 10.0 wt%, and 15.0 wt%, manifesting a decrease of 25.60%, 32.30%, and 40.60% for  $R_C$  and 3.40%, 4.10%, and 4.90% for mass, respectively. This work provides sufficient evidence that surplus sludge has a huge potential application for building materials from the perspective of improving their mechanical properties. It provides an important theoretical basis for the disposal as well as efficient utilization of sludge.



**Citation:** Liang, J.; He, H.; Wei, J.; Han, T.; Wang, W.; Wang, L.; Han, J.; Zhang, L.; Zhang, Y.; Ma, H. Study of Solidifying Surplus Sludge as Building Material Using Ordinary Portland Cement. *Processes* **2022**, *10*, 2234. <https://doi.org/10.3390/pr10112234>

Academic Editors: Hayet Djelal, Abdeltif Amrane and Nabila Khellaf

Received: 9 October 2022

Accepted: 28 October 2022

Published: 31 October 2022

**Publisher's Note:** MDPI stays neutral with regard to jurisdictional claims in published maps and institutional affiliations.



**Copyright:** © 2022 by the authors. Licensee MDPI, Basel, Switzerland. This article is an open access article distributed under the terms and conditions of the Creative Commons Attribution (CC BY) license (<https://creativecommons.org/licenses/by/4.0/>).

**Keywords:** surplus sludge; solidification; unconfined compression strength; ordinary Portland cement

## 1. Introduction

The surplus sludge is produced as a solid precipitate in the municipal wastewater treatment processes, such as physical separation or the gravitational precipitation process [1]. The amount of surplus sludge has been escalating worldwide at an alarming rate with an increase in the amount of municipal sewage due to the rapid development of population,

urbanization, industrialization, sewage drainage systems, and wastewater treatment facilities [2–6]. Commonly, the surplus sludge contains four kinds of compounds, apart from moisture [4,7–9], heavy metals [1–4,8–12]; organic and inorganic compounds [2,3,8,9,11–14]; microorganisms, such as *E. coli*, *Salmonella* spp., and *Enterococcus* [1–4,8,10–14]; and solid granules [8,12], which are harmful to soil, vegetation, animals, and humans [3,4,11,15–19]. Conventional treatment methods for treating surplus sludge, such as landfilling, deposition into the ocean, and composting, are being phased out due to their ecotoxicological risks and the concerns raised by the public and environmentalists regarding the potential toxicity of untreated sewage sludge to the environment [2–4,17]. The development of more cutting-edge treatment technologies is urgent.

The newer surplus sludge treatment methods can be divided into three types, namely, thermal treatment [4,17,18,20–22], biological treatment [1,14,23–27], and chemical treatment [2,4,19,28,29]. The following metrics can be used to evaluate how well various sludge treatment techniques perform: carbon or nitrogen recovery, volume/weight reduction, pathogen elimination, and stabilization of heavy metals or organic matter [1,2]. Thermal treatments such as pyrolysis, incineration, gasification, hydrothermal carbonization, or supercritical water gasification are effective for weight reduction, and could convert the carbon into biofuels while consuming less energy [1,2,30]. Although it takes longer, the biological treatment uses less energy to recover carbon [1]. However, in China, these methods are hardly ever used. Until 2016, China used about 25% of its surplus sludge for composting and material recovery [1,7].

Solidification/stabilization (S/S) technology is an important method at present in the disposal of solid waste, which could limit the release of harmful chemicals into the environment [31–33]. The contaminants are chemically bound during the stabilization process and mechanically bound during the solidification process [31]. This method was initially applied for the management of sludge and later for soil remediation [32]. The S/S technology has attracted the attention of many remediation practitioners due to its capacity to accomplish rapid remedial objectives at a comparatively low cost [32], so that leftover sludge can be transformed into a type of building material using S/S technology. One of the primary cementing materials for conventional S/S technology is ordinary Portland cement, which is widely accessible and reasonably priced [33].

In this work, ordinary Portland cement was used to solidify the surplus sludge for comprehensive utilization. The unconfined compressive strength ( $R_C$ ) was mainly used to assess the possibility of application in the building materials field. The fly ash and sodium silicate ( $\text{Na}_2\text{SiO}_3$ ) were added to the surplus sludge solidification process to improve the  $R_C$ . The effects of the ratio of liquid to solid ( $R_{l/s}$ ), surplus sludge dosage ( $D_S$ ), dosages of sodium silicate ( $D_{\text{Na}_2\text{SiO}_3}$ ) and fly ash ( $W_F$ ), and the sodium silicate modulus (molar ratio of  $\text{SiO}_2$  to  $\text{Na}_2\text{O}$  in sodium silicate, shorted as  $M$ ) on the  $R_C$  of cement–surplus sludge solidified blocks (hereafter referred to as solidified blocks) were investigated. The solidified blocks were characterized by scanning electron microscopes (SEM), X-ray Diffraction Analysis (XRD), and Fourier transform-infrared spectroscopy (FT-IR). To investigate the effect of environmental temperature on the mechanical properties of solidified blocks, the freeze-thaw cycling experiment was carried out. Cement–surplus sludge solidified blocks fabricated in this work have been designed to furnish enough mechanical strength for use as a building material and for utilization in a low-temperature environment. This work would provide a theoretical basis for the application of surplus sludge in building materials.

## 2. Experiments

### 2.1. Materials

The surplus sludge used in the solidification experiment was obtained from the Haicheng wastewater treatment plant in Liaoning province (China). Industrial grade ordinary Portland cement (P.O. 42.5) was purchased from Fushun Da Huang Cement Co., China (Fushun, China). Analytical grade sodium silicate ( $\text{Na}_2\text{SiO}_3$ ) was purchased

from Shanghai Rhawn Chemical Technology Co. (Shanghai, China), with the modulus varying in the range of 1.00–2.43. Fly ash was purchased from Henan Gongyi Longze Water Purification Material Co. (Gongyi City, China). The ingredients are listed in Table 1. Fly ash and  $\text{Na}_2\text{SiO}_3$  were used as received. Deionized water was obtained from a Hitech-Kflow water purification system (Hitech Co., Beijing, China).

**Table 1.** Ingredient of fly ash supplied by corresponding companies.

Chemical Composition	Weight (wt%)	Chemical Composition	Weight (wt%)
$\text{SiO}_2$	53.97	$\text{MgO}$	1.01
$\text{Al}_2\text{O}_3$	31.15	$\text{Na}_2\text{O}$	0.89
$\text{Fe}_2\text{O}_3$	4.16	$\text{SO}_3$	0.73
$\text{CaO}$	4.01	$\text{P}_2\text{O}_5$	0.67
$\text{K}_2\text{O}$	2.04	$\text{Cl}$	0.13
$\text{TiO}_2$	1.13	$\text{NiO}$	0.11

## 2.2. Property Analysis of Surplus Sludge

Using a mass-loss technique, the moisture and organic components in surplus sludge were examined. The surplus sludge was dried for 12 h at 105 °C in an oven (Shanghai Jinghong Experimental Equipment Co., Shanghai, China), using a mount ( $m_0 = 20.0$  g) placed in a culture dish. The surplus sludge was then chilled in a drier. The mass of the leftovers was measured ( $m_1$ ). The water content ( $w_w$ ), which can be determined using the Formula (1), was the mass removed from the sludge throughout this procedure. The organic mass ( $m_2$ ) in the remaining dry sludge was reduced in weight by calcining it at 600 °C for 3 h without using a lid in a muffle furnace (Resistance Furnace Temperature Controller, Shaoxing Shangyu Road market branch analysis instrument factory, China), and the organic content ( $w_o$ ) can be calculated using the Formula (2). The amount of residue ( $w_a$ ) in surplus sludge can be calculated using Formula (3). The findings showed that the surplus sludge contained 84.6 wt% water, 10.8 wt% residues, and 29.9 wt% organic material (amounting to 29.9 wt% in dry surplus sludge).

$$w_w = \frac{m_0 - m_1}{m_0} \times 100\% \quad (1)$$

$$w_o = \frac{m_2}{m_0} \times 100\% \quad (2)$$

$$w_a = 1 - w_w - w_o \quad (3)$$

The total organic carbon (TOC) value of dry surplus sludge was 25.4 wt%, which was measured by the MultiN/C 3100 TOC instrument (Jena, Germany), and was consistent with the result from the calcination method.

The pH value of surplus sludge was measured according to a standard of determination method for municipal sludge in wastewater treatment plants (CJ/T 221-2005) [34]. About 5.0 g surplus sludge was placed in a 200 mL glass bottle, 50.0 mL of deionized water was added to it, and the bottle was covered with a cap. The mixture was then shaken in a THZ-82 thermostatic water bath shaker (Wuhan Grey Mo Lai Detection Equipment Co., Wuhan, China) at 270 cycles·min<sup>−1</sup> at 25.0 °C for 4 h and then deposited for 48 h at room temperature. By using the electrode method, the pH of the supernatant was determined to be 7.3, which is the pH of the surplus sludge.

## 2.3. Solidification Experiment of the Surplus Sludge

The surplus sludge in this solidification experiment was pre-treated by having the water removed by being heated at 105 °C for 16 h before being solidified. The dry surplus sludge was then broken up using a 1.0 mm sieve and a DS-1 high-speed tissue masher (Shanghai Specimen Model Factory Co., Shanghai, China) and sifted using a sieve with an

aperture of 1.0 mm. Then, a given amount of the powdered filter residue powder was mixed and then combined with a predetermined quantity of ordinary Portland cement,  $\text{Na}_2\text{SiO}_3$ , or fly ash. The solid mixtures were mixed with deionized water at a mass ratio of liquid to solid ( $R_{l/s}$ ) of 0.35–0.55 using a YD90S-8/4 cement mortar mixer (Wuxi Construction Engineering Test Equipment Co., Wuxi, China) for 20 min to obtain a cement mixed mortar. The solid mixtures were mixed with deionized water at a mass ratio of liquid to solid ( $R_{l/s}$ ) of 0.35–0.55 to create a cement mixed mortar. The designed solidification experimental scheme is shown in Table 2. Table 2 displays the planned solidification experimental plan. In the table, the designed surplus sludge dosage ( $D_s$ ) varied in the range of 0.0–15.0 wt% in the solid mixtures. The designed surplus sludge dosage ( $D_s$ ) in the solid mixtures ranged from 0.0 wt% to 15.0 wt% in the table. The dosage of  $\text{Na}_2\text{SiO}_3$  ( $D_{\text{Na}_2\text{SiO}_3}$ ) and the proportion of fly ash varied in the range of 0.0–9.0 wt% and 0.0–15.0 wt%. The cement mix mortar was shaken in a shaking table for 20 min to remove air bubbles, and then poured into a cubic plexiglass mold with an inner diameter of 40 mm  $\times$  40 mm  $\times$  40 mm, purchased from the Fushun Plexiglass factory. The cement mix mortar in the cubic plexiglass mold was cured for 3–60 days at room temperature to form the solidified blocks. The unconfined compression strength ( $R_C$ ) of solidified blocks was measured using a compression testing machine (Jinan Dong Fang Test Instrument Co., Jinan, China), for which the loading rate was  $2400 \pm 200$  N/s. The  $R_C$  can be calculated using the following Formula (4).

$$R_C = F_C / A \quad (4)$$

where  $F_C$  is the maximum load at failure, of which the unit is N.  $A$  is the pressure area with the unit of  $\text{mm}^2$  (40 mm  $\times$  40 mm).

**Table 2.** Experiment scheme of cement solidified residual sludge.

Solidified Block	$D_S/\text{wt}\%$	$D_P/\text{wt}\%$	$R_{l/s}$	$D_{\text{Na}_2\text{SiO}_3}/\text{wt}\%$	M	$W_F/\text{wt}\%$
DS0	0.0	100.0	0.35	0.0	-	0.0
			0.45			
			0.55			
DS5	5.0	95.0	0.35	0.0	-	0.0
			0.45			
			0.55			
DS10	10.0	90.0	0.35	0.0	-	0.0
			0.45			
			0.55			
DS15	15.0	85.0	0.35	0.0	-	0.0
			0.45			
			0.55			
B3S0	0.0	100.0	0.45	3.0	2.43	0.0
B3.0			3.0			
B4.5			4.5			
B6.0	5.0	95.0	0.45	6.0	2.43	0.0
B7.5				7.5		
B9.0				9.0		
F5.0	5.0	90.0	0.45	-	-	5.0
F10.0		85.0				10.0
F15.0		80.0				15.0
F20.0		75.0				20.0
F25.0		70.0				25.0
F15S0	0.0	85.0	0.45	-	-	15.0

$D_p$ ,  $D_s$ , and  $D_{\text{Na}_2\text{SiO}_3}$  were the mass proportion of ordinary Portland cement, surplus sludge, and  $\text{Na}_2\text{SiO}_3$  in solid phase, respectively.

#### 2.4. Freeze-Thaw Recycle Experiment

The freeze-thaw recycle experiment was designed to investigate the effect of temperature ( $T$ ) on unconfined compressive strength ( $R_C$ ). The solidified blocks were prepared

according to Table 3 and cured for 28 days at room temperature. After that, the solidified blocks were immersed in water and put into a freeze-thaw cycle testing machine ( machine, Nanjing Jiedi Electronic Equipment Manufacturing Co., Nanjing, China) to evaluate the freeze-thaw cycle. After an initial drop in temperature from 8 °C to −18 °C within 60 min, the temperature stayed that way for another 60 min before rising to 8 °C. A freeze-thaw cycle is used and takes 4 h. A freeze-thaw cycle temperature diagram is shown in Figure 1. The solidified blocks A-C in Table 3 underwent freeze-thaw cycles of 0–50. Every 10 freeze-thaw cycles, the mass and  $R_C$  of solidified block samples were measured.

**Table 3.** Freeze-thaw recycle experiment scheme.

Sample	$D_{Na_2SiO_3}/wt\%$	$D_S/wt\%$	$D_P/wt\%$	M	$W_F/wt\%$	$R_{I/s}$
A	7.5	5.0	75.0	1.00	20.0	0.35
B	7.5	10.0	70.0	1.00	20.0	0.35
C	7.5	15.0	65.0	1.00	20.0	0.35

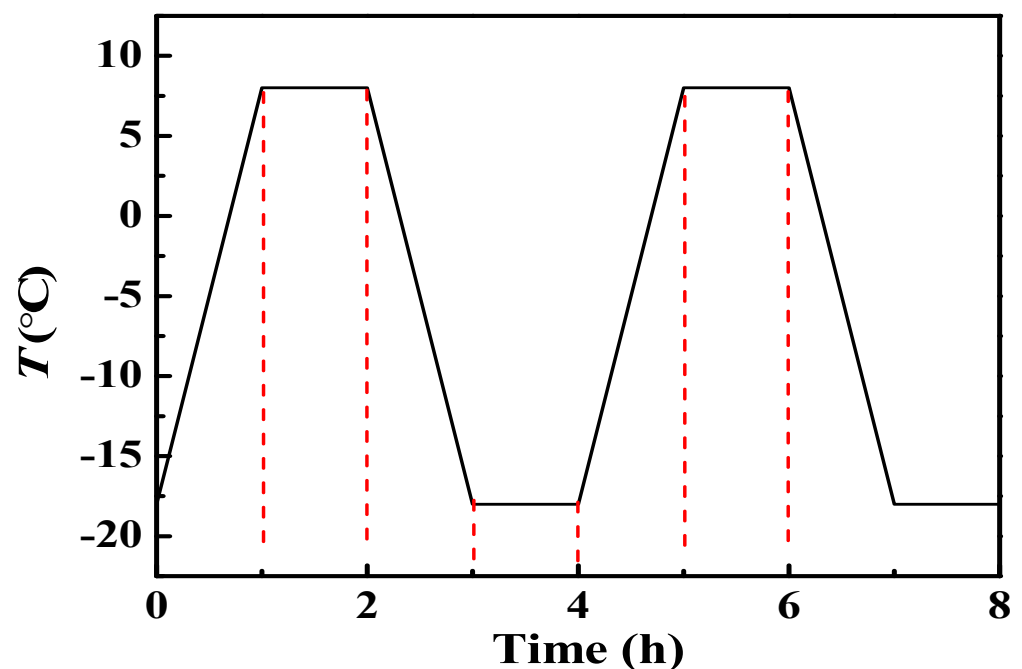


**Figure 1.** Freeze-thaw cycle temperature diagram.

In all the above experiments, each test was conducted in triplicate, and the final  $R_C$  values were an average of the three measurements. For comparison, blank tests were performed for the Portland cement in the absence of the surplus sludge. The solidified blocks of DS0, B3S0, and F15S0 are the blank samples for investigating the effects of  $D_{Na_2SiO_3}$  and  $W_F$  on the  $R_C$  of the Portland cement solidified blocks.



### 2.5. Characterization

The prepared solidified blocks were crushed using a compression testing machine (Jinan Dong Fang Test Instrument Co., Jinan, China) and the specimen was collected. Then, the specimen was ground to powder. The powder sample was characterized by scanning electron microscopy (SEM), X-ray diffraction (XRD), and Fourier transform infrared (FT-IR) spectra. The morphologies of solidified block samples were observed using scanning electron microscope imaging (SEM, Supra 55, Zeiss, Jena, Germany). Crystal structures were determined by powder X-ray diffraction (XRD), using a D/max-rA model diffractometer (Bruker Co., Germany) with Cu K $\alpha$  radiation ( $\lambda = 1.54184 \text{ \AA}$ ) operating at 40 kV and 40 mA. Fourier transform infrared (FT-IR) spectra were recorded using a Vertex 70 model infrared spectrometer (Bruker Co., Hanau, Germany) using standard KBr discs.

## 3. Results and Discussion

### 3.1. The Characterization of Surplus Sludge and Solidified Blocks

The surplus sludge was solidified by the Portland cement with mechanical strength. Figure 2 shows the images of the prepared solidified blocks. Solidified blocks rarely shrank or expanded in volume.

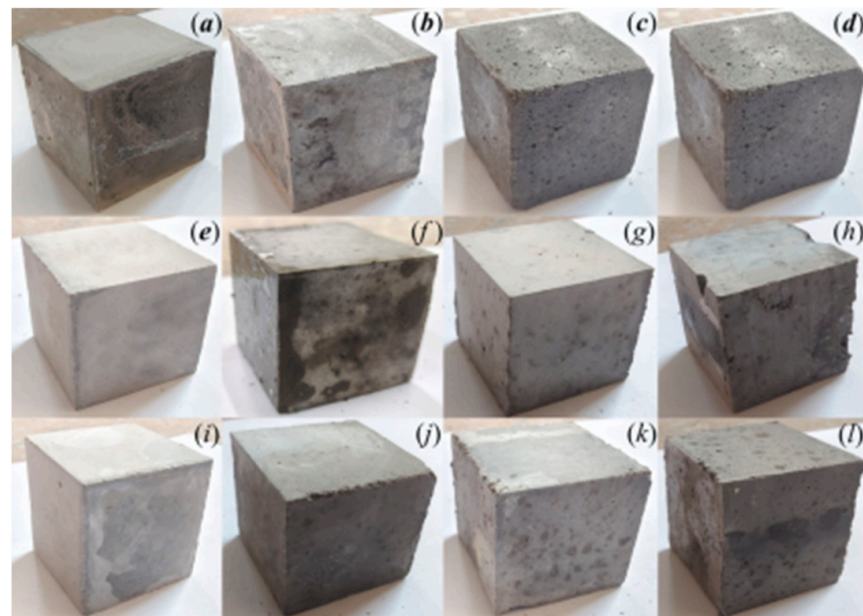


**Figure 2.** The photos of the solidified blocks at  $R_{1/s} = 0.45$ . (a–d) are DS0, DS5, DS10, and DS15; (e–h) are B3S0, B4.5, B7.5, and B9 samples; (i–l) are F15S0, F5.0, F10.0, and F15.0.

#### 3.1.1. FTIR Spectra of Raw Materials and Solidified Blocks

Figure 3a presents the FTIR spectra of the surplus sludge ash residue, dry surplus sludge, fly ash, and  $\text{Na}_2\text{SiO}_3$ . The peaks at  $3432 \text{ cm}^{-1}$ ,  $1650 \text{ cm}^{-1}$ , and  $1451 \text{ cm}^{-1}$  in the spectrum of surplus sludge may be attributed to the asymmetric stretching vibration and bending vibration of the O-H bond of crystalline hydrate existing within the surplus sludge [35,36]. The two absorption peaks at  $2923 \text{ cm}^{-1}$  and  $2852 \text{ cm}^{-1}$  are the characteristic absorptions of the asymmetric and symmetric C-H and  $-\text{CH}_2-$  bonds, which may arise from the carbon skeleton of various organic compounds that formed the sludge [37,38]. The absorption peaks at  $3432 \text{ cm}^{-1}$ ,  $2923 \text{ cm}^{-1}$ ,  $2852 \text{ cm}^{-1}$ ,  $1650 \text{ cm}^{-1}$ , and  $1451 \text{ cm}^{-1}$  are weakened in the spectrum for the surplus sludge ash because most of the organics and crystalline hydrate were burned out mostly at  $600^\circ\text{C}$ . The wide peak at about  $1004\text{--}1094 \text{ cm}^{-1}$  is the asymmetric vibration of the Si-O-T (T is Si or Al) bond from the  $\text{SiO}_2$  and  $\text{Al}_2\text{O}_3$  contained in the raw materials [35,38]. The absorption peaks at  $556 \text{ cm}^{-1}$

and  $539\text{ cm}^{-1}$  may be assigned to Fe-O lattice vibrations, and the peak at  $463\text{ cm}^{-1}$  is Si-O bending vibration [35,38]. These Fe-O and Si-O bonds may form from the Fe flocculating agent and sandstone contained in surplus sludge.

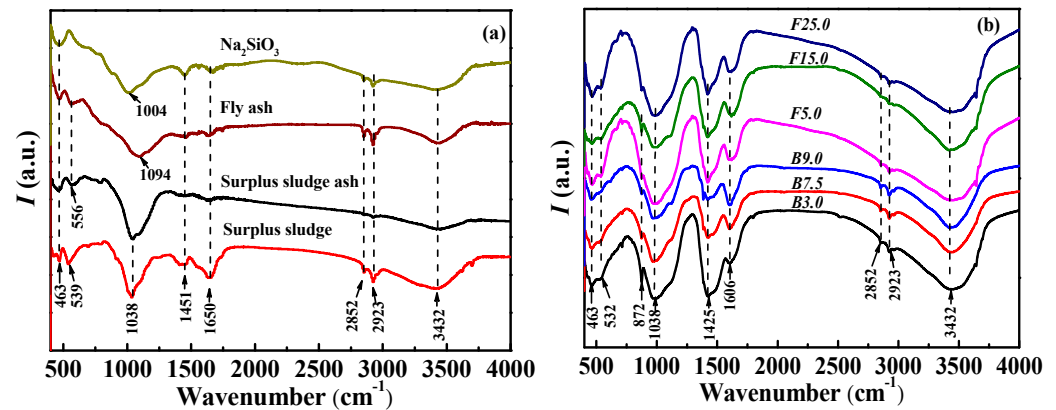


**Figure 3.** (a) is FTIR spectra of the ash residuum of surplus sludge and raw materials; (b) is FTIR spectra of solidified blocks.

In Figure 3b, the absorptions peaks of  $3432\text{ cm}^{-1}$ ,  $2923\text{ cm}^{-1}$ ,  $2852\text{ cm}^{-1}$ ,  $539\text{ cm}^{-1}$ , and  $463\text{ cm}^{-1}$  in surplus sludge appeared in the infrared spectra of B3.0, B7.5, B9.0, F5, F15, and F25 samples. It demonstrated that surplus sludge was solidified in cement solidified blocks. The asymmetric stretching vibration, in-plane, and out-of-plane vibrations, and bending vibration of the O-H bond of crystalline hydrate existent in surplus sludge–cement solidified blocks from hydration reaction is responsible for the peaks at  $1606\text{ cm}^{-1}$  and  $1425\text{ cm}^{-1}$ , respectively [35,36]. The results are consistent with the reports [35].

### 3.1.2. SEM Micrographs of Solidified Blocks

Figure 4 represents the SEM micrographs of raw materials and solidified blocks. Figure 4a–c show the sludge was a clumped granular structure, the Portland cement solidified blocks (DS0) mainly existed as a lamellar structure, whereas the fly ash manifested a faveolate structure. While image Figure 4d presents flake-like structures, indicating the surplus sludge was solidified by cement. When  $\text{Na}_2\text{SiO}_3$  was added during the solidification process, the lamellar structure from Portland cement solidified blocks was unchanged, as shown in Figure 4e. The images in Figure 4f–h show that the large block structure was gradually replaced by small compact block structures with the increase in dosage of  $\text{Na}_2\text{SiO}_3$ . Compared with the image presented in Figure 4c, a thick rod crystal and acicular crystal appeared in the image in Figure 4i. In photo Figure 4j, the dry surplus sludge was wrapped by a faveolate structure, lamellar structure, and a long rodlike structure. Several clavate structures appear in sample F10.0 (Figure 4k). The degree of fragmental block structure increases in sample F15.0 (Figure 4l).

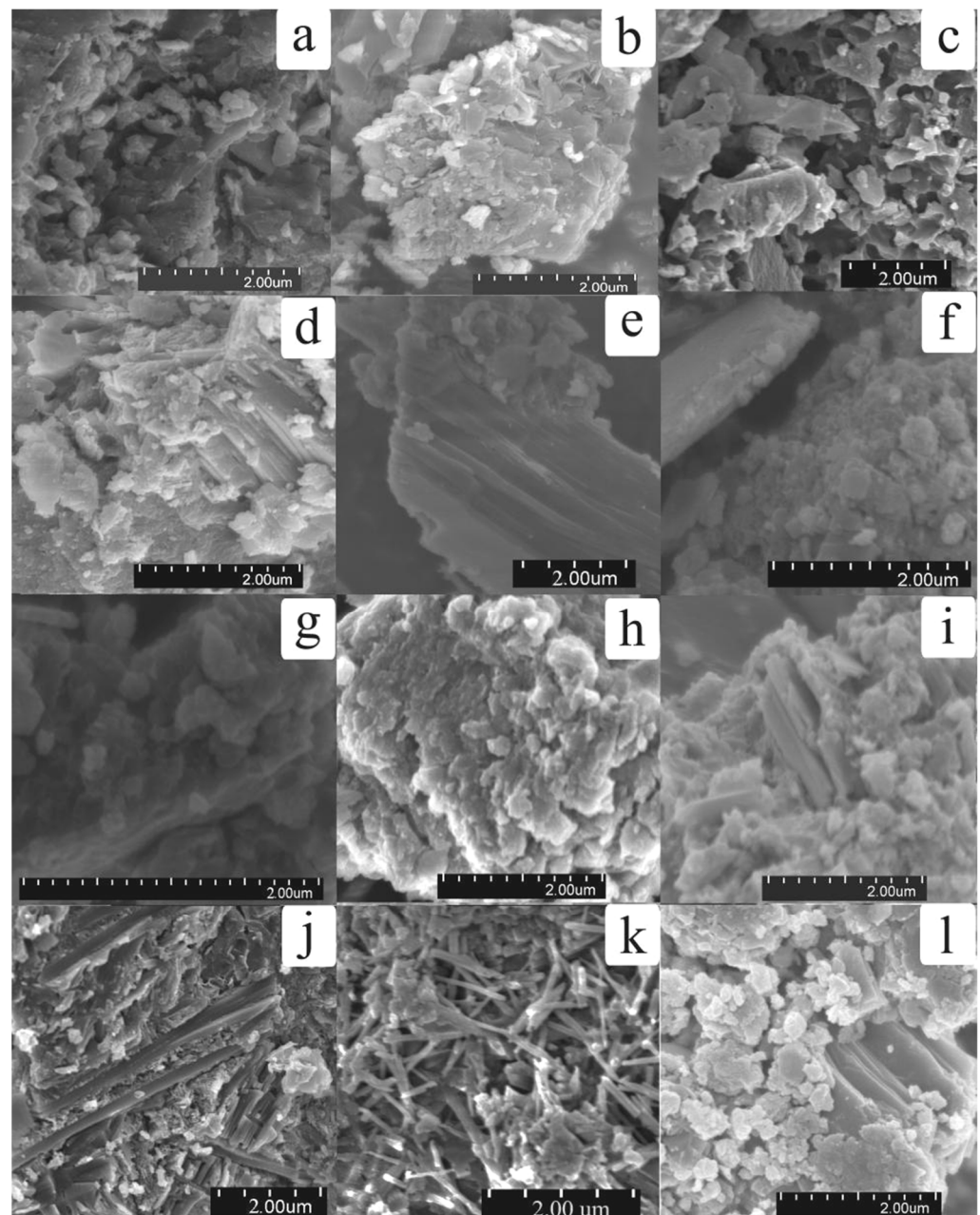


**Figure 4.** SEM photographs of raw materials and solidified blocks curing for 60 days. (a) dry surplus sludge, (b) DS0 sample ( $R_{1/s} = 0.45$ ), (c) fly ash, (d) DS5 ( $R_{1/s} = 0.45$ ), (e) B3S0, (f–h) are B4.5, B7.5, and B9.0 samples, respectively, (i–l) are F15S0, F5.0, F10.0, and F15.0 samples, respectively.

### 3.1.3. X-ray Diffraction Analysis (XRD) of Solidified Blocks

Figure 5 is the XRD diffraction spectra of the solidified blocks. It is shown that the principal components of the solidified blocks were  $\text{SiO}_2$ , aluminosilicate, and  $\text{CaCO}_3$ . The results were consistent with the previous research [35,39,40]. Aluminosilicate maybe consisted of the calcium silicate hydrate (C-S-H) and calcium aluminate hydrate (C-A-H).



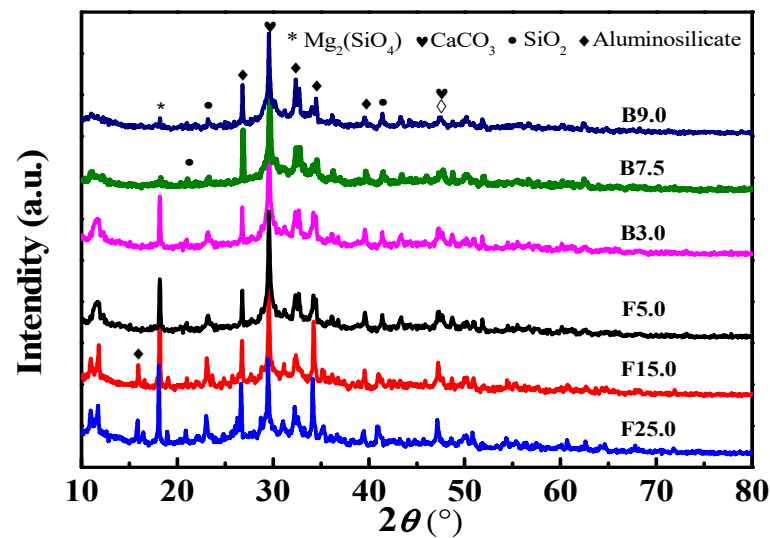


Figure 5. XRD pattern of cement–surplus sludge solidified blocks.

### 3.2. Effects of $D_s$ and $R_{l/s}$ on $R_C$ of Solidified Blocks

Figure 6 shows the effects of surplus sludge dosage ( $D_s$ ) and the ratio of liquid to solid ( $R_{l/s}$ ) on the unconfined compressive strength ( $R_C$ ) of solidified blocks. The  $R_C$  reached the equilibrium value at about 28 days for Figure 6a and at 60 days for Figure 6b–d. The reason was that the substitution of surplus sludge for some of the Portland cement reduced the curing rate and required more time to form the strength phase than solidified blocks made entirely of Portland cement.

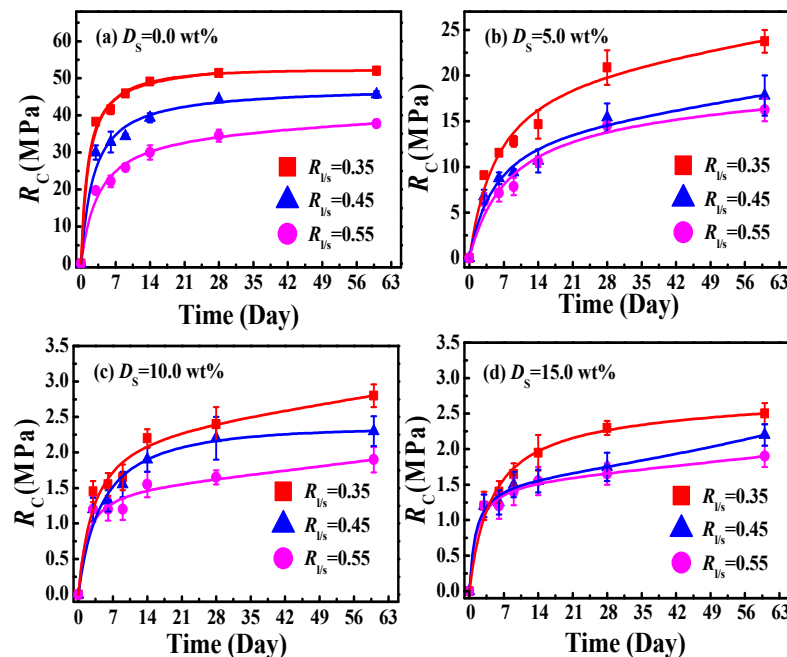


Figure 6. The effects of  $D_s$  and  $R_{l/s}$  on  $R_C$  of solidified blocks at room temperature. (a) is the  $R_C$  of blank samples of Portland cement solidified blocks. (b–d) are the  $R_C$  of cement–surplus sludge solidified blocks with different  $D_s$ .

Compared with  $R_C$  of Portland cement solidified blocks, Figure 6 also shows that  $R_C$  reduced with  $R_{l/s}$  increasing at a given  $D_s$  and reduced with  $D_s$  increasing from 0.0 wt% to 15.0 wt% when  $R_{l/s}$  varied in the range of 0.35–0.55. For instance,  $R_C$  of 60 days reduced to 23.75 MPa from 52.05 MPa at  $R_{l/s} = 0.35$  when  $D_s$  increased to 5.0 wt% from

0.0 wt%, reducing by a total of 54.37%. Furthermore, the  $R_C$  reduced with  $R_{1/s}$  increasing from 0.35 to 0.55 at the given  $D_S$ .  $R_C$  of 60 days reduced from 2.80 MPa to 1.90 MPa with the increase in  $R_{1/s}$  from 0.35 to 0.55, when  $D_S$  was 10.0 wt%. There was no obvious difference for  $R_C$  before 28 days at  $R_{1/s} = 0.45$  and 0.55 when  $D_S$  was 15.0 wt%. Due to the hydration-produced gelling material such as  $\text{Ca}(\text{OH})_2$ , calcium silicate hydrate (C-S-H, clavate), and calcium aluminate hydrate (C-A-H, microcrystalline gel), which wrapped the surplus sludge, in this work, Portland cement was the main cementitious materials to form the strength of solidified blocks. Additionally, when solidified blocks were cured at room temperature, a portion of the  $\text{Ca}(\text{OH})_2$  gel that was present in the hydrated cement slurry may react with  $\text{CO}_2$  in the atmosphere and change into  $\text{CaCO}_3$ , and XRD diffraction spectra revealed the presence of  $\text{CaCO}_3$  (seen in Figure 5). As a result, as  $D_S$  increased,  $R_C$  decreased, and as the curing time was extended,  $R_C$  increased. The Portland cement dosage was thus decreased as  $D_S$  increased due to the fact that the amount of gel material decreases and hydration was diminished as  $D_S$  increased. It was challenging to obtain saturation with the  $\text{Ca}(\text{OH})_2$ , calcium silicate hydrate (C-S-H) and hydrated cement slurry to prevent the formation of stable crystal or insoluble when the water concentration was too high. Therefore, the  $R_C$  reduced with  $R_{1/s}$  increasing.

### 3.3. The Effect of $\text{Na}_2\text{SiO}_3$ on $R_C$ of Solidified Blocks

It was reported that sodium silicate ( $\text{Na}_2\text{SiO}_3$ ) is one of the common alkali activators of geopolymers with better mechanical properties and durability [35]. So, how sodium silicate affected the unconfined compression strength ( $R_C$ ) of solidified blocks was examined. First, the effect of the molar ratio (M) of  $\text{SiO}_2$  to  $\text{Na}_2\text{O}$  in sodium silicate on the  $R_C$  of the solidified blocks was investigated, as shown in Figure 7. Results indicated that adding  $\text{Na}_2\text{SiO}_3$  hastened the curing process and the  $R_C$  of 28 days gradually approached the equilibrium value. Furthermore, the  $R_C$  of 60 days increased initially and then reduced with M increasing from 1.00 to 2.43.  $R_C$  of 60 days reached the maximum value of 28.00 MPa when M was 1.70,  $D_S$  was 5.0 wt%, and  $R_{1/s}$  was 0.45. Compared with DS5 ( $R_{1/s} = 0.45$ , 17.80 MPa) without  $\text{Na}_2\text{SiO}_3$ ,  $R_C$  of 60 days was 25.90 MPa, 27.10 MPa, 28.00 MPa, 24.05 MPa, and 23.10 MPa, raising by 45.51%, 52.25%, 57.30%, 35.11%, and 29.78%; in turn, when M was 1.00, 1.35, 1.70, 2.05, and 2.43. The results are similar to those mentioned previously in the literature report, that is, when the modulus value and dosage of sodium silicate were under appropriate conditions, the strength increased [35,41]. The addition of  $\text{Na}_2\text{SiO}_3$  was therefore advantageous for improving  $R_C$ .

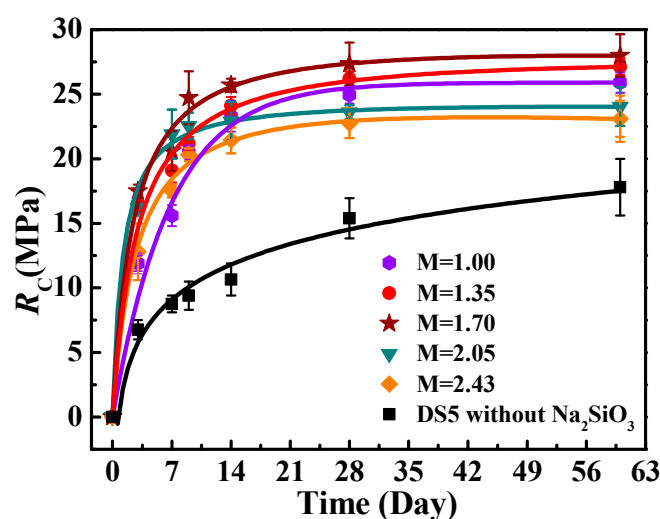


**Figure 7.** The effect of modulus of sodium silicate on  $R_C$  of 28 days for solidified blocks solidified at room temperature at the  $R_{1/s} = 0.45$ ,  $D_{\text{Na}_2\text{SiO}_3} = 9.0$  wt% and  $D_S = 5.0$  wt%.

The effect of  $D_{\text{Na}_2\text{SiO}_3}$  on  $R_C$  was also investigated when  $D_S$  was 5.0 wt%,  $R_{1/s}$  was 0.45, and  $M$  was 2.43, as shown in Figure 8. The  $R_C$  of 28 days steadily approached the equilibrium value because the addition of  $\text{Na}_2\text{SiO}_3$  could speed up the curing process, which was consistent with Figure 7. With  $D_{\text{Na}_2\text{SiO}_3}$  increasing from 0.0 wt% to 9.0 wt%,  $R_C$  of 28 and 60 days increased initially and then reduced. Generally,  $R_C$  was better than the  $R_C$  of sample DS5 ( $R_{1/s} = 0.45$ ) and  $R_C$  was improved. The possible explanations are as follows: (1) the  $\text{Na}_2\text{SiO}_3$  could increase the proportion of C-S-H during the cement slurry curing process; and (2) in the aqueous solution,  $\text{Na}_2\text{SiO}_3$  hydrolysis would produce some spherical  $\text{SiO}_2$  particles, as shown in Figure 5, improving the strength of solidified blocks. With  $D_{\text{Na}_2\text{SiO}_3}$  increasing from 0.0 wt% to 7.5 wt%, the  $R_C$  of 60 days increased from 17.80 MPa to 34.70 MPa, an increase of 94.94%.  $R_C$  of 60 days reduced from 34.70 MPa to 23.95 MPa with  $D_{\text{Na}_2\text{SiO}_3}$  increasing from 7.5 wt% to 9.0 wt%, which was increased by 34.55% all the same compared with the  $R_C$  of DS5 ( $R_{1/s} = 0.45$ ). At  $D_{\text{Na}_2\text{SiO}_3} = 7.5$  wt%,  $R_C$  of 60 days reached the highest value of 34.70 MPa, which was approached  $R_C$  (35.95 MPa) for the B3S0 sample (see Figure S1 in the Supporting information) without surplus sludge. When  $D_{\text{Na}_2\text{SiO}_3}$  was 9.0 wt%, the degree of growth on  $R_C$  of 60 days was lower. It may be the acceleration in hydration reaction caused by the increase in alkalinity, resulting in  $\text{Ca}(\text{OH})_2$  and calcium silicate hydrate (C-S-H) being produced in the hydration reaction process, failing to fill pores in time.

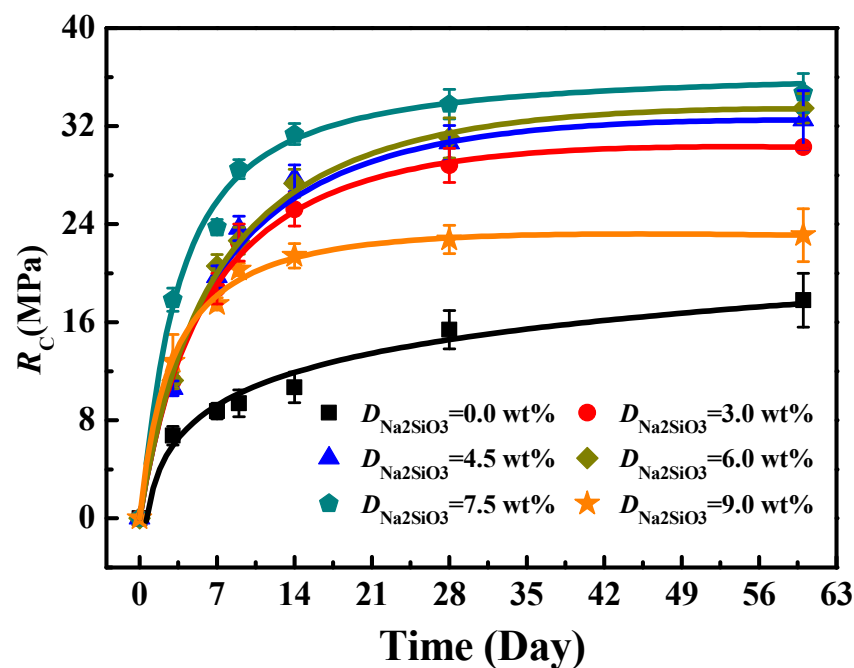


**Figure 8.** The effect of  $D_{\text{Na}_2\text{SiO}_3}$  on  $R_C$  of solidified blocks at room temperature when  $R_{1/s}$  was 0.45,  $D_S$  was 5.0 wt%, and  $M$  was 2.43.

When  $D_S$  reached 5.0 wt%, the  $R_C$  over 30.29 MPa was sufficient from a mechanical strength perspective for comprehensive utilization of the surplus sludge as a building material. While the amount of surplus sludge utilized was less for higher mechanical strength.

### 3.4. The Effect of Fly Ash on $R_C$ of Solidified Blocks

As known, fly ash, usually produced in the coal burning process, could improve the performance of Portland cement [35]. Therefore, to investigate the effect of fly ash on the unconfined compression strength ( $R_C$ ) of solidified blocks, fly ash was added to the solidifying process. Figure 9 shows the effect of fly ash dosage ( $W_F$ ) on  $R_C$  at room temperature cured for 60 days when  $R_{1/s}$  was 0.45 and  $D_S$  was 5.0 wt%. The results show

that  $R_C$  of 60 days increased initially and then reduced with  $W_F$  increasing from 0.0 wt% to 25.0 wt%. When  $W_F$  was 10.0 wt%,  $R_C$  of 60 days reached the highest value of 34.35 MPa. From 0.0 wt% to 10.0 wt% of  $W_F$ ,  $R_C$  increased to 34.35 MPa from 17.80 MPa, increasing overall by 92.98%. While  $W_F$  increased from 10.0 wt% to 25.0 wt%,  $R_C$  reduced to 20.30 MPa from 34.35 MPa, thereby demonstrating a rise of 14.04% in comparison with the sample of  $W_F = 0.0$  wt% (DS5, 17.80 MPa). It indicated that adding fly ash might increase the solidified body made of sludge and cement's mechanical strength, with 10.0 wt% of fly ash being the ideal amount. According to Table 1, the fly ash had higher concentrations of  $\text{SiO}_2$ ,  $\text{Al}_2\text{O}_3$ ,  $\text{Fe}_2\text{O}_3$ , and  $\text{CaO}$ , which led to the production of more calcium silicate hydrates (C-S-H), calcium aluminate hydrates (C-A-H), and ettringite being produced [36,37], which were used to continuously fill the fly ash's honeycomb pores during the cement curing process. As a result, during the cement's hydration and hardening processes, a dense solid was generated. Moreover, clavate (C-S-H) and fragmental structures (C-A-H) were observed in Figure 4j–l.

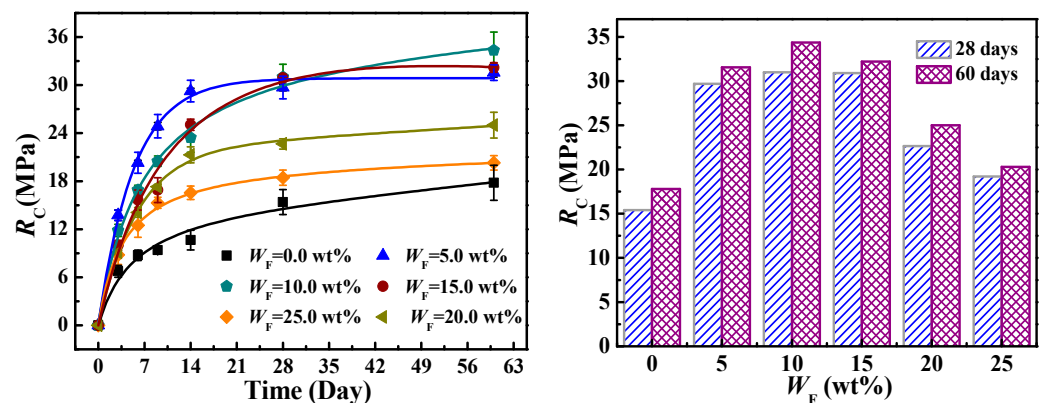


**Figure 9.** The effect of  $W_F$  on  $R_C$  of solidified blocks at room temperature cured for 60 days when the  $R_{I/s}$  was 0.45 and the  $D_S$  was 5 wt%.

In addition, when  $R_{I/s}$  was 0.35, the  $R_C$  of 60 days was 23.75 MPa and only 2.50 MPa when  $D_S$  was 5.0 wt% and 15.0 wt%, respectively. The utilization of sludge dosage ( $D_S$ ) was still lower for solidified blocks with relatively higher mechanical properties (>20 MPa). The  $\text{Na}_2\text{SiO}_3$  and fly ash have the potential to improve the mechanical strength of sludge–cement based solidified blocks. Hence, the effect of  $\text{Na}_2\text{SiO}_3$  and fly ash on the  $R_C$  of sludge–cement based solidified bodies with different  $D_S$  was investigated according to the Table 3 to improve the mechanical strength of sludge–cement-based solidified blocks with higher  $D_S$ . The result is shown in Figure 10.  $R_C$  reduced with an increase in  $D_S$ , such that the  $R_C$  of 28 days was 40.69 MPa, 32.60 MPa, and 26.70 MPa when  $D_S$  was 5.0 wt%, 10.0 wt%, and 15.0 wt%, raising by 94.97%, about 13 times and about 10 times, respectively, compared with the  $R_C$  of 28 days of sludge–cement based solidified blocks without  $\text{Na}_2\text{SiO}_3$  and fly ash. At this ratio, the utilization of sludge dosage ( $D_S = 15.0$  wt%) with higher mechanical strength (>20 MPa) was increased by double compared with  $D_S = 5.0$  wt% ( $R_{I/s} = 0.35$ ).

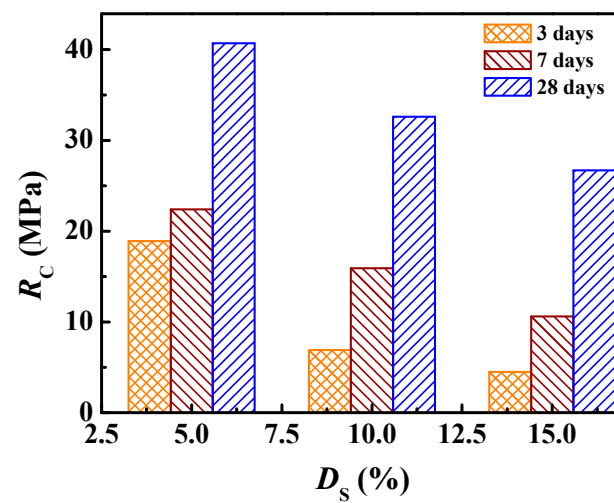


**Figure 10.** The effect of  $\text{Na}_2\text{SiO}_3$  ( $M = 1.00$ ) and fly ash on the  $R_c$  of sludge–cement–based solidified blocks with different  $D_s$  at room temperature cured for 28 days when the  $R_{l/s}$  was 0.35.

### 3.5. The Effect of Freeze-Thaw Cycling on the $R_c$ of Solidified Blocks

The effect of temperature ( $T$ ) on  $R_c$  was also investigated through the freeze-thaw recycle experiment shown in Figure 11. The mass loss of solidified blocks could reflect the degree of damage to solidified blocks. The results show that the mass of solidified blocks increased initially and then reduced with the increase in the number of freeze-thaw cycles, which is consistent with literature reports [42]. After a total of 50 freeze-thaw cycles, the mass reduced by 3.4%, 4.1%, and 4.9% when  $D_s$  was 5.0 wt%, 10.0 wt%, and 15.0 wt%, respectively, indicating that the mass loss rate increased with  $D_s$  increasing. In the early stage of the freeze-thaw cycling experiment, the phenomenon of an increase in the mass of solidified blocks with the increase in the number of freeze-thaw cycles was caused by the formation of new pores in the solidified blocks, leading to a large amount of water migrating inside. When the number of freeze-thaw cycles increased to a certain value, the pore water in the solidified blocks gradually accumulated due to volume expansion in the freezing process. Slowly, cracks developed internally within the solidified blocks and were squeezed, making it difficult for water to enter the inside, and the water sublimated or volatilized more and more, resulting in an increased mass loss.

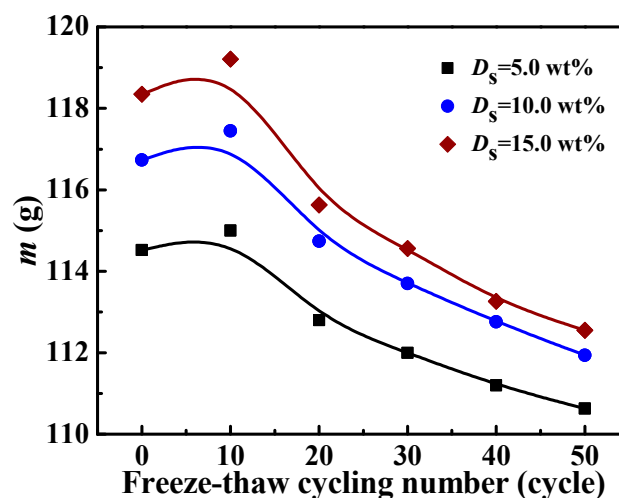


**Figure 11.** The effect of freeze-thaw cycling number on mass of sludge–cement–based solidified blocks with different  $D_s$  when  $R_{l/s}$  was 0.35,  $D_{\text{Na}_2\text{SiO}_3}$  was 7.5%, and  $W_F$  was 20.0 wt%.



The freeze-thaw cycling experiment was carried out to investigate the effect of temperature ( $T$ ) on unconfined compression strength ( $R_C$ ). Figure 12 shows the effect of the number of freeze-thaw cycles on the  $R_C$  of sludge–cement based solidified blocks with different  $D_S$  when the  $R_{1/s}$  was 0.35,  $D_{Na_2SiO_3}$  was 7.5 wt%, and  $W_F$  was 20.0 wt%. The results show that  $R_C$  decreased linearly with  $D_S$  and increased with the number of freeze-thaw cycles, reducing by 25.6%, 32.3%, and 40.6% after a total of 50 freeze-thaw cycles for  $D_S$  of 5.0 wt%, 10.0 wt%, and 15.0 wt%, respectively. Lower temperatures (below 0 °C) would cause the liquid water in the solidified blocks to change into the solid phase, resulting in an expansion in the volume. Figure 13 depicts this expansion in volume. The pores were produced as the solid water liquified to the liquid phase. Transverse expansion and vertical contraction would take place on the surface of solidified blocks when a vertical force is applied to them. The pores would connect throughout the freeze-thaw recycle operations, in turn, resulting in fissures inside the solidified blocks. The transverse crack was closed when the solidified block was subjected to vertical pressure, however, the more vertical cracks were produced as the fracture stress increased, resulting in a sizable reduction in  $R_C$ . The crack-changing mechanism has been depicted in Figure 14.

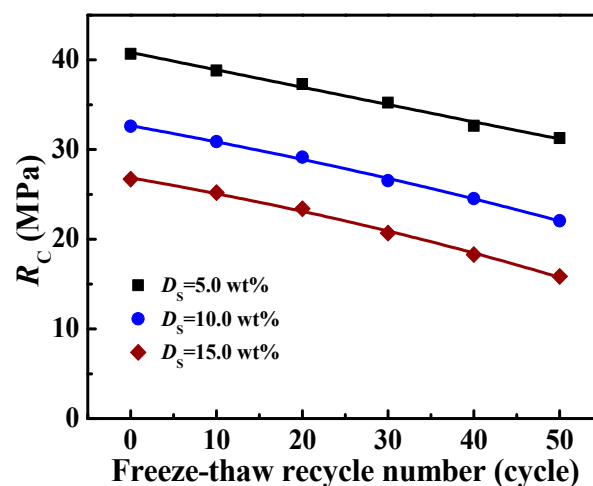


**Figure 12.** The effect of the number of freeze-thaw cycles on  $R_C$  of sludge–cement-based solidified blocks with different  $D_S$  when  $R_{1/s}$  was 0.35,  $D_{Na_2SiO_3}$  was 7.5%, and  $W_F$  was 20 wt%.

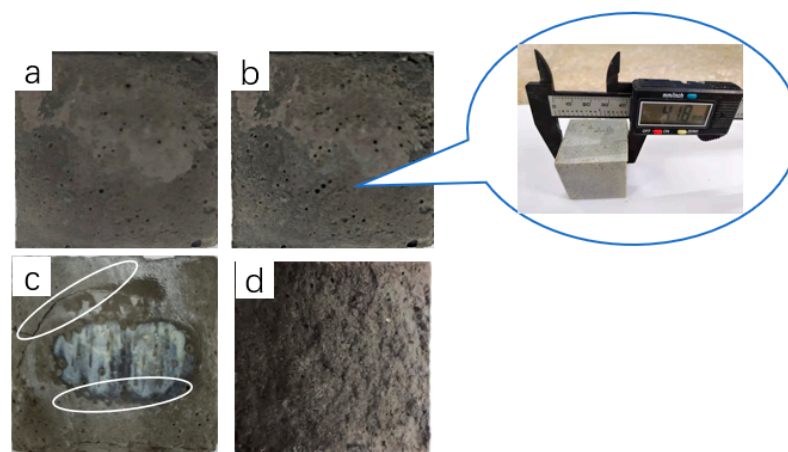


**Figure 13.** Deterioration diagram after freeze-thaw cycles of 0–50 when  $D_S$  was 15.0 wt%, (a) 0 freeze-thaw cycle; (b) 10 freeze-thaw cycles; (c) 20 freeze-thaw cycles; (d) 30–50 freeze-thaw cycles.

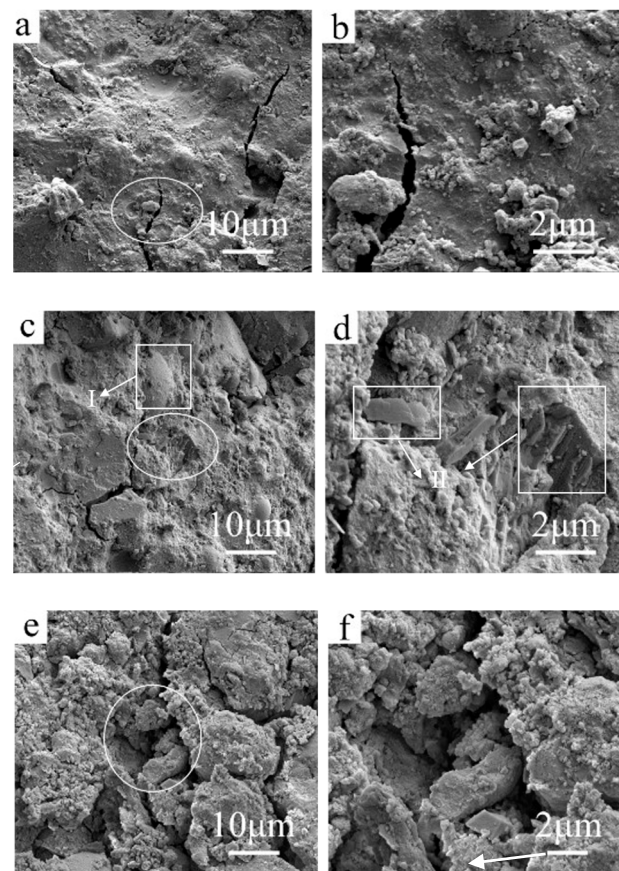


**Figure 14.** SEM photographs of solidified blocks with  $D_S = 15\%$ . Number of freeze-thaw cycles of: (a,b) were 10 cycles; (c,d) were 30 cycles; (e,f) were 50 cycles. Photographs (b,d,f) are the enlarge the pictures of (a,c,e) respectively.

Figure 14 shows the SEM photographs of solidified blocks with a  $D_S$  of 15.0 wt% and a 10–50 freeze-thaw cycle. Figure 14b,d,f are the enlarged images of Figure 14a,c,e, respectively. Figure 14a,b show that the cracks were produced in the solidified blocks after 10 freeze-thaw cycles. Figure 14c,d show that the surface of the solidified block becomes rough, the crack becomes wide and some particles are shed from the surface of the solidified block. While Figure 14e,f demonstrate how the crack collapsed and the solidified block became loose. There were, thus, more pores were produced. All of the aforementioned findings show how the crack eventually collapses, diminishing unconfined compression strength ( $R_C$ ) with the increase in the number of freeze-thaw cycles.

#### 4. Conclusions

Using regular Portland cement, surplus sludge from sewage treatment plants was solidified to investigate the potential for application in construction materials from the standpoint of mechanical properties. The effects of  $R_{1/s}$ , surplus sludge dosage ( $D_S$ ), curing time (Time), dosage of sodium silicate ( $D_{Na_2SiO_3}$ ), and fly ash ( $W_F$ ) on the unconfined compression strength ( $R_C$ ) of cement–surplus sludge solidified blocks were investigated. The FTIR spectra of cement–surplus sludge solidified blocks indicated that the surplus sludge was solidified by cement, and the photographs of solidified blocks show that solidified blocks hardly shrank or dilated in volume. The  $R_C$  reached the equilibrium value at about 60 days for cement–surplus sludge solidified blocks.  $R_C$  reduced with  $R_{1/s}$  increasing at the given  $D_S$  and was reduced with  $D_S$  increasing from 0.0 wt% to 15.0 wt% at  $R_{1/s}$  of 0.35–0.55. The addition of  $Na_2SiO_3$  and fly ash could improve the  $R_C$  of the solidified blocks.  $R_C$  increased initially and then reduced with  $D_{Na_2SiO_3}$  increasing from 0.0 wt% to 9.0 wt% at  $R_{1/s} = 0.45$  when  $D_S$  was 5.0 wt% and  $M = 2.43$ . The  $R_C$  of 60 days reached the

highest value of 34.70 MPa when  $D_{\text{Na}_2\text{SiO}_3}$  was 7.5 wt%.  $R_C$  increased initially and then reduced, with  $W_F$  increasing to 25.0 wt% from 0.0 wt%. When  $W_F$  was 15.0 wt%, the  $R_C$  of 60 days reached the highest value of 34.35 MPa, rising by 93.8% when  $W_F$  was 10.0 wt%. At the ratio of  $D_{\text{Na}_2\text{SiO}_3}$  of 7.50 wt%,  $R_{1/5}$  of 0.35,  $W_F$  of 20.0 wt%,  $D_S$  of 15.0 wt%, and  $M$  of 1.00,  $R_C$  reached 26.70 MPa, increasing by about 10 times in comparison with that of sludge–cement based solidified blocks without  $\text{Na}_2\text{SiO}_3$  and fly ash. At this ratio, the utilization of sludge utilized ( $D_S = 15.0$  wt%) was increased by twice compared with  $D_S = 5.0$  wt%. Through a freeze–thaw cycling experiment, the impact of environmental temperature on the mechanical characteristics of the solidified block was also investigated. For solidified blocks with  $D_S$  of 5.0 wt%, 10.0 wt%, and 15.0 wt%, respectively, the  $R_C$  and mass were reduced with the freeze–thaw cycle number increasing from 10 to 50 cycles. According to this study, surplus sludge has the desired mechanical properties to be used as a building material. It provides an important theoretical foundation for the efficient disposal and comprehensive utilization of surplus sludge through solidification/stabilization technology using ordinary Portland cement.

**Supplementary Materials:** The following supporting information can be downloaded at: <https://www.mdpi.com/article/10.3390/pr10112234/s1>, Figure S1: The effect of sodium silicate and fly ash on the RC at room temperature when the RI/s was 0.45.

**Author Contributions:** Conceptualization, J.L. and H.H.; methodology, H.H. and J.W.; software, T.H.; validation, L.W.; formal analysis, W.W.; investigation, H.M.; resources, L.Z. and Y.Z.; data curation, J.L.; writing—original draft preparation, J.L.; writing—review and editing, J.L.; visualization, J.W.; supervision, J.H.; project administration, L.Z.; funding acquisition, J.L. All authors have read and agreed to the published version of the manuscript.

**Funding:** This research was funded by China College Students Innovation and Entrepreneurship Fund [No. 202110148018] and Talent Scientific Research Fund of Liaoning Petrochemical University [No. 2016xJJ-031]. And the APC was funded by J. Liang.

**Conflicts of Interest:** The authors declare they have no known conflict of interest or personal relationships influencing the work reported in this paper.

## References

1. Liew, C.S.; Yunus, N.M.; Chidi, B.S.; Lam, M.K.; Goh, P.S.; Mohamad, M.; Sin, J.C.; Lam, S.M.; Lim, J.W.; Lam, S.S. A review on recent disposal of hazardous sewage sludge via anaerobic digestion and novel composting. *J. Hazard. Mater.* **2022**, *423*, 126995. [CrossRef] [PubMed]
2. Liew, C.S.; Kiatkittipong, W.; Lim, J.W.; Lam, M.K.; Ho, Y.C.; Ho, C.D.; Ntwampe, S.K.O.; Mohamad, M.; Usman, A. Stabilization of heavy metals loaded sewage sludge: Reviewing conventional to state-of-the-art thermal treatments in achieving energy sustainability. *Chemosphere* **2021**, *277*, 130310. [CrossRef]
3. Wei, L.; Zhu, F.; Li, Q.; Xue, C.; Xia, X.; Yu, H.; Zhao, Q.; Jiang, J.; Bai, S. Development, current state and future trends of sludge management in China: Based on exploratory data and  $\text{CO}_2$ -equivalent emissions analysis. *Environ. Int.* **2020**, *144*, 106093. [CrossRef] [PubMed]
4. Liu, X.; Zhai, Y.; Li, S.; Wang, B.; Wang, T.; Liu, Y.; Qiu, Z.; Li, C. Hydrothermal carbonization of sewage sludge: Effect of feed-water pH on hydrochar's physicochemical properties, organic component and thermal behavior. *J. Hazard. Mater.* **2020**, *388*, 122084. [CrossRef] [PubMed]
5. Sun, Y.; Chen, Z.; Wu, G.; Wu, Q.; Zhang, F.; Niu, Z.; Hu, H.Y. Characteristics of water quality of municipal wastewater treatment plants in China: Implications for resources utilization and management. *J. Clean. Prod.* **2016**, *131*, 1–9. [CrossRef]
6. Wang, T.; Shi, F.; Zhang, Q.; Qian, X.; Hashimoto, S. Exploring material stock efficiency of municipal water and sewage infrastructures in China. *J. Clean. Prod.* **2018**, *181*, 498–507. [CrossRef]
7. Zhang, Q.H.; Yang, W.N.; Ngo, H.H.; Guo, W.S.; Jin, P.K.; Dzakupasu, M.; Yang, S.J.; Wang, Q.; Wang, X.C.; Ao, D. Current status of urban wastewater treatment plants in China. *Environ. Int.* **2016**, *92–93*, 11–22. [CrossRef]
8. Dong, B.; Liu, X.; Dai, L.; Dai, X. Changes of heavy metal speciation during high-solid anaerobic digestion of sewage sludge. *Bioresour. Technol.* **2013**, *131*, 152–158. [CrossRef]
9. Breulmann, M.; van Afferden, M.; Müller, R.A.; Schulz, E.; Fühner, C. Process conditions of pyrolysis and hydrothermal carbonization affect the potential of sewage sludge for soil carbon sequestration and amelioration. *J. Anal. Appl. Pyrolysis* **2017**, *124*, 256–265. [CrossRef]
10. Al-Gheethi, A.A.; Efaq, A.N.; Bala, J.D.; Norli, I.; Abdel-Monem, M.O.; Kadir, M.O.A. Removal of pathogenic bacteria from sewage-treated effluent and biosolids for agricultural purposes. *Appl. Water Sci.* **2018**, *8*, 74. [CrossRef]

11. Yang, G.; Zhang, G.; Wang, H. Current state of sludge production, management, treatment and disposal in China. *Water Res.* **2015**, *78*, 60–73. [[CrossRef](#)] [[PubMed](#)]
12. Anders, A.; Weigand, H.; Cakir, H.; Kornhaas, U.; Platen, H. Phosphorus recycling from activated sludge of full-scale wastewater treatment plants by fast inversion of the biological phosphorus elimination mechanism. *J. Environ. Chem. Eng.* **2021**, *9*, 106403. [[CrossRef](#)]
13. Shehu, M.S.; Abdul Manan, Z.; Alwi, S.R. Optimization of thermo-alkaline disintegration of sewage sludge for enhanced biogas yield. *Bioresour. Technol.* **2012**, *114*, 69–74. [[CrossRef](#)] [[PubMed](#)]
14. Zhang, G.; Yang, J.; Liu, H.; Zhang, J. Sludge ozonation: Disintegration, supernatant changes and mechanisms. *Bioresour. Technol.* **2009**, *100*, 1505–1509. [[CrossRef](#)]
15. Fijalkowski, K.; Rorat, A.; Grobelak, A.; Kacprzak, M.J. The presence of contaminations in sewage sludge—the current situation. *J. Environ. Manag.* **2017**, *203*, 1126–1136. [[CrossRef](#)]
16. Peng, C.; Zhai, Y.; Zhu, Y.; Xu, B.; Wang, T.; Li, C.; Zeng, G. Production of char from sewage sludge employing hydrothermal carbonization: Char properties, combustion behavior and thermal characteristics. *Fuel* **2016**, *176*, 110–118. [[CrossRef](#)]
17. Suarez-Iglesias, O.; Urrea, J.L.; Oulego, P.; Collado, S.; Diaz, M. Valuable compounds from sewage sludge by thermal hydrolysis and wet oxidation—A review. *Sci. Total Environ.* **2017**, 584–585, 921–934. [[CrossRef](#)]
18. Wang, T.; Zhai, Y.; Zhu, Y.; Li, C.; Zeng, G. A review of the hydrothermal carbonization of biomass waste for hydrochar formation: Process conditions, fundamentals, and physicochemical properties. *Renew. Sustain. Energy Rev.* **2018**, *90*, 223–247. [[CrossRef](#)]
19. Wei, L.; Li, J.; Xue, M.; Wang, S.; Li, Q.; Qin, K.; Jiang, J.; Ding, J.; Zhao, Q. Adsorption behaviors of Cu<sup>2+</sup>, Zn<sup>2+</sup> and Cd<sup>2+</sup> onto proteins, humic acid, and polysaccharides extracted from sludge EPS: Sorption properties and mechanisms. *Bioresour. Technol.* **2019**, *291*, 121868. [[CrossRef](#)]
20. Hii, K.; Baroutian, S.; Parthasarathy, R.; Gapes, D.J.; Eshtiaghi, N. A review of wet air oxidation and thermal hydrolysis technologies in sludge treatment. *Bioresour. Technol.* **2014**, *155*, 289–299. [[CrossRef](#)]
21. Manara, P.; Zabanitoutou, A. Towards sewage sludge based biofuels via thermochemical conversion—A review. *Renew. Sustain. Energy Rev.* **2012**, *16*, 2566–2582. [[CrossRef](#)]
22. Werle, S.; Wilk, R.K. A review of methods for the thermal utilization of sewage sludge: The polish perspective. *Renew. Energy* **2010**, *35*, 1914–1919. [[CrossRef](#)]
23. Anjum, M.; Al-Makishah, N.H.; Barakat, M.A. Wastewater sludge stabilization using pre-treatment methods. *Process Saf. Environ.* **2016**, *102*, 615–632. [[CrossRef](#)]
24. Appels, L.; Baeyens, J.; Degreè, J.; Dewil, R. Principles and potential of the anaerobic digestion of waste-activated sludge. *Prog. Energy Combust. Sci.* **2008**, *34*, 755–781. [[CrossRef](#)]
25. Wei, L.; Qin, K.; Ding, J.; Xue, M.; Yang, C.; Jiang, J.; Zhao, Q. Optimization of the co-digestion of sewage sludge, maize straw and cow manure: Microbial responses and effect of fractional organic characteristics. *Sci. Rep.* **2019**, *9*, 2374. [[CrossRef](#)]
26. Yang, D.; Hu, C.; Dai, L.; Liu, Z.; Dong, B.; Dai, X. Post-thermal hydrolysis and centrate recirculation for enhancing anaerobic digestion of sewage sludge. *Waste Manag.* **2019**, *92*, 39–48. [[CrossRef](#)]
27. Zhao, X.; Kumar, K.; Gross, M.A.; Kunetz, T.E.; Wen, Z. Evaluation of revolving algae biofilm reactors for nutrients and metals removal from sludge thickening supernatant in a municipal wastewater treatment facility. *Water Res.* **2018**, *143*, 467–478. [[CrossRef](#)]
28. Wang, Y.; Zhou, Y.T.; Feng, D.; Wu, C.L.; Wang, X.; Min, F.L. Effect of chemical conditioners on deep dewatering of urban dewatered sewage sludge in the temporary sludge lagoon. *J. Environ. Eng.* **2019**, *145*, 04019063. [[CrossRef](#)]
29. Wei, L.; Xia, X.; Zhu, F.; Li, Q.; Xue, M.; Li, J.; Sun, B.; Jiang, J.; Zhao, Q. Dewatering efficiency of sewage sludge during Fe<sup>2+</sup>-activated persulfate oxidation: Effect of hydrophobic/hydrophilic properties of sludge EPS. *Water Res.* **2020**, *181*, 115903. [[CrossRef](#)]
30. Ge, S.; Foong, S.Y.; Ma, N.L.; Liew, R.K.; Mahari, W.A.W.; Xia, C.; Yek, P.N.Y.; Peng, W.; Nam, W.L.; Lim, X.Y.; et al. Vacuum pyrolysis incorporating microwave heating and base mixture modification: An integrated approach to transform biowaste into eco-friendly bioenergy products. *Renew. Sustain. Energy Rev.* **2020**, *127*, 109871. [[CrossRef](#)]
31. Xu, Z.; Ye, D.; Dai, T.; Dai, Y. Research on preparation of coal waste-based geopolymer and its stabilization/solidification of heavy metals. *Integr. Ferroelectr.* **2021**, *217*, 214–224. [[CrossRef](#)]
32. Shen, Z.; Jin, F.; O'Connor, D.; Hou, D. Solidification/stabilization for soil remediation: An old technology with new vitality. *Environ. Sci. Technol.* **2019**, *53*, 11615–11617. [[CrossRef](#)]
33. Tuncan, A.; Tuncan, M.; Koyuncu, H. Use of petroleum-contaminated drilling wastes as sub-base material for road construction. *Waste Manag. Res.* **2000**, *18*, 489–505. [[CrossRef](#)]
34. Ministry of Construction of the People's Republic of China. *Determination Method for Municipal Sludge in Wastewater Treatment Plant*; Ministry of Construction of the People's Republic of China: Beijing, China, 2005. (In Chinese)
35. Lv, Q.; Yu, J.; Ji, F.; Gu, L.; Chen, Y.; Shan, X. Mechanical property and microstructure of fly ash-based geopolymer activated by sodium silicate. *KSCE J. Civ. Eng.* **2021**, *25*, 1765–1777. [[CrossRef](#)]
36. Kowalski, M.; Kowalska, K.; Wiszniowski, J.; Turek-Szytow, J. Qualitative analysis of activated sludge using FT-IR technique. *Chem. Pap.* **2018**, *72*, 2699–2706. [[CrossRef](#)]

37. Ma, J.; Li, P.; Wang, W.; Wang, S.; Pan, X.; Zhang, F.; Li, S.; Liu, S.; Wang, H.; Gao, G.; et al. Biodegradable poly (amino acid)-gold-magnetic complex with efficient endocytosis for multimodal imaging-guided chemo-photothermal therapy. *ACS Nano* **2018**, *12*, 9022–9032. [[CrossRef](#)]
38. Barbosa, V.F.F.; MacKenzie, K.J.D.; Thaumaturgo, C. Synthesis and characterisation of materials based on inorganic polymers of alumina and silica: Sodium polysialate polymers. *Int. J. Inorg. Mater.* **2000**, *2*, 309–317. [[CrossRef](#)]
39. Yakubu, Y.; Zhou, J.; Ping, D.; Shu, Z.; Chen, Y. Effects of pH dynamics on solidification/stabilization of municipal solid waste incineration fly ash. *J. Environ. Manag.* **2018**, *207*, 243–248. [[CrossRef](#)]
40. Li, J.T.; Zeng, M.; Ji, W.X. Characteristics of the cement-solidified municipal solid waste incineration fly ash. *Environ. Sci. Pollut. Res.* **2018**, *25*, 36736–36744. [[CrossRef](#)]
41. Hou, Y.F.; Wang, D.M.; Li, Q.; Lu, H.B. Effect of water glass performance on fly ash-based geopolymers. *J. Chin. Ceram. Soc.* **2008**, *36*, 61–64. (In Chinese) [[CrossRef](#)]
42. Li, J.L.; Zhu, L.Y.; Zhou, K.P.; Liu, H.W.; Cao, S.P. Damage characteristics of sandstone pore structure under freeze-thaw cycles. *Rock Soil Mech.* **2019**, *40*, 3524–3532. (In Chinese)